Research paper

Influence of charge diameter on detonation velocity and reaction zone of ANFO explosive contained in a steel tube

Naoki Kinoshita*, Shiro Kubota**, Tei Saburi**, Yuji Ogata**, and Atsumi Miyake*†

*Graduate School of Environment and Information Sciences, Yokohama National University,
79-7, Tokiwadai, Hodogaya-ku, Yokohama 240-8501, JAPAN
TEL : +81-45-339-3993, FAX : +81-45-339-4011
†Corresponding address atsumi@ynu.ac.jp

**Research Core for Explosion Safety, National Institute of Advanced Industrial Science and Technology,
16-1, Onogawa, Tsukuba 305-8569, JAPAN
e-mail kubota.46@aist.go.jp

Received : October 4, 2010 Accepted : January 17, 2011

Abstract

To obtain a better understanding of the detonation properties of non-ideal explosives containing ammonium nitrate as the main ingredient, numerical simulations of the detonation of ammonium nitrate and fuel oil mixture (ANFO) are implemented using an Eulerian hydrocode, and compared with the experimental results of an ANFO steel tube test. The simulation results of the detonation velocity at various charge diameters accord with experimental ones. The simulations also showed that the shock front in the detonation wave in ANFO is slightly curved. The profiles for the mass fraction of detonation products differ according to the position in the charge and the dimension of the charge diameter.

Keywords : ANFO, non-ideal detonation, numerical simulation, Eulerian hydrocode, diameter effect

1. Introduction

Ammonium nitrate (AN) has been extensively used as the main component in industrial explosives. It is well known that explosives containing AN exhibit non-ideal detonation behavior. This non-ideality of detonation is manifested in our experiments as the dependence of the detonation velocity on experimental conditions such as the diameter of the explosive charge, the confinement conditions, and the discrepancy of the detonation velocity from its ideal value[1].

We have studied non-ideal detonation behavior for various types of AN-based explosives. One of the authors[2,3] has carried out investigations into pure AN using large diameter steel tubes, and predicted the detonation velocity in the case of an infinite diameter. Many co-workers[4-7] have performed experiments to understand the effect on the detonation velocity of the diameter of the charge, the strength of confinement, and the substances used in the explosives. The detonation of condensed phase matter is a high-velocity phenomenon and brings about extremely high pressures and temperatures, which makes it very difficult to conduct precise experiments. Therefore, research that combines experiments and numerical analysis is an effective approach. In order to understand the non-ideal behavior of explosives, many useful numerical approaches have been proposed, and numerical research has been progressed in this area. We will seek an understanding of non-ideal behavior from the viewpoints of experiments and numerical analysis.

In this study, numerical simulations of non-ideal detonation of ammonium nitrate and fuel oil mixture (ANFO) are implemented using an Eulerian hydrocode. The simple and useful reaction rate model and the mixture rule have been employed in the hydrocode. The previously obtained diameter-effect data of ANFO are represented by numerical simulations, and we discuss those results on the non-ideal behavior of ANFO

Table 1 The parameters of the equations of state for ANFO (initial density 904 kg m^{-3}) and its detonation properties. JWL isentrope ; $P_S = A\exp(-R_1\eta) + B\exp(-R_2\eta) + C\eta^{-(\omega+1)}, \eta = V/V_0$

Murnaghan EOS parameters					
ρ_0 [kgm^{-1}]	C_0 [ms^{-1}]	n [−]	k [Pa^{-1}]		
904	681	7.4	238×10^{-11}		
JWL parameters*					
E_0 [Jkg^{-1}]	A [Pa]	B [Pa]	C [Pa]	R_1 [−]	R_2 [−]
4.27×10^{6}	1.45×10^{11}	1.99×10^{9}	8.9×10^{8}	5.01	1.03
ω [−]	P_{CJ} [Pa]	V_{CJ} [m^{3}kg^{-1}]	D_{CJ} [ms^{-1}]	C_{CJ} [ms^{-1}]	
0.33	5.83×10^{9}	8.11×10^{-4}	4914	3601	

explosives.

2. Numerical simulation

2.1 Numerical procedure

To simulate the detonation of an explosive, a reaction rate equation and equations of state (EOS) are required in addition to the governing equations of fluid. We adopted the method proposed by Souers[8], which consists of the simple equations explained below. The EOS for an unreacted explosive and the detonation products are the Murnaghan equation, and the JWL isentrope, respectively. The Murnaghan equation is as follows.

$$P = \frac{1}{nk}\left(\frac{V_0}{V} - 1\right). \tag{1}$$

Where V is the specific volume and subscript 0 indicate the initial condition. The parameters n and k are the constant. The parameters for Murnaghan EOS and JWL isentrope are shown in Table 1.

The mixture rule for the unreacted explosive and the reaction product is the following equation,

$$P = (1-F)P_e + FP_p. \tag{2}$$

The reaction rate of explosive is represented by the following equation,

$$\frac{dF}{dt} = G\,(P+q)^b(1-F). \tag{3}$$

where P is pressure, F is mass fraction of detonation products, q is artificial viscosity, t is time, and G and b are reaction rate parameters. Subscripts e and p denote unreacted explosive and detonation products, respectively.

These equations were incorporated into a two−dimensional Eulerian hydrocode developed by Explosion Safety Core at AIST[9)−11)]. The hydrocode has advantageous features for the calculation of detonation and shock phenomena owing to the adoption of a Eulerian scheme, the CIP (cubic−interpolated propagation) method and Vorobiev's pressure calculation method.

2.2 Simulation conditions

The geometry of the system for our numerical simulation is illustrated in Fig. 1. The conditions in the simulations are set so as to be the same as in our previous

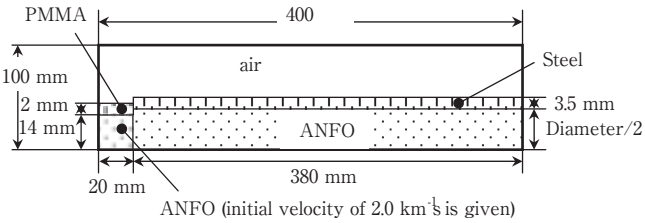

Fig. 1 Initial geometrical condition for the simulation.

detonation velocity measurement experiments on ANFO. The ANFO charge is confined in a cylindrical steel tube, which is regarded as having axial symmetry in the simulation. In the experiment, the ANFO charges are of various diameters, namely 27, 35, and 42 mm, whereas the thickness of the wall of the steel tubes is fixed at 3.5 mm, and this is also the case in the simulations. The initial density of the ANFO is 904 kg m^{-3} in all cases. The ANFO charge is initiated at one end, from which the detonation wave propagates to the other end. In the simulations, at one end of the ANFO charge, a pellet of ANFO of somewhat high density (1040 kg m^{-3}) is positioned and given an initial velocity of 2.0 km s^{-1} toward the main ANFO charge so as to represent initiation by a powerful booster charge. In each case, the same initiation conditions are used.

The CFL (Courant−Friedrichs−Lewy Condition) number is set to 0.1. The grid size is set to 0.5 mm, and the number of grid squares is 801 for the direction parallel to the axis, and 201 for the direction perpendicular to the axis. As the EOS for the steel tube, the Mie−Gruneisen equation is adopted. The confinement tube is surrounded by air at atmospheric pressure. The boundary condition applied is a continuous boundary, except for the axis of the axisymmetric coordinate for which a reflective boundary is applied.

In the simulations, the values of the coefficient G and the pressure exponent b in Eq.(2) are varied simultaneously to fit the simulated detonation velocity to the experimentally obtained values. The JWL and Murnaghan parameters required for the simulation are determined using the thermodynamic code CHEETAH 2.0. The values of parameters used in the simulation are listed in Table 1.

Table 2 Comparison with simulation and experimental detonation properties of ANFO.

Diameter [mm]	Experiment	Simulation (b=2.0, G=400)		
	Detonation velocity [kms^{-1}]	Detonation velocity [kms^{-1}]	Axial position	Detonation driving zone length [mm]
27	3.43	3.50	Central	5.5
			Peripheral	5.5
36	3.66	3.56	Central	5.5
			Peripheral	5.0
42	3.78	3.66	Central	5.5
			Peripheral	5.0

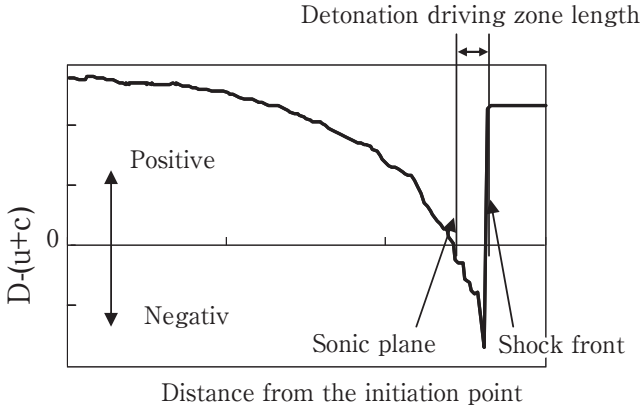

Fig. 2 The conceptual diagram for the definition of the Detonation driving zone (distribution of the D−(u+c), D −(u+c)=0is a sonic plane).

2.3 Detonation driving zone

The perturbation generated by chemical reaction within the domain between the leading shock front and the sonic plane contributes to a propagation of the steady state detonation wave. In the sonic plane, the following relation among detonation velocity D, local sound speed c, and particle velocity u, is to be held when a coordinate system moving with the shock front is adopted,

$$D = c + u. \tag{4}$$

Transforming Eq.(4), the relation $D-(c + u)=0$ is obtained. In this study, as illustrated in Fig. 2, the sonic point is defined as the position where the value of $D-(c + u)$ is 0, and the detonation driving zone length is defined as the distance between the shock front and the sonic plane. The detonation driving zone length differs from the so−called reaction zone length, but corresponds to the effective reaction zone length. Sound speed c is calculated simply by differentiating Eq.(2).The relation between detonation velocity and the detonation driving zone is discussed later in this study.

3. Results and discussion

The parameters b and G for the reaction rate were examined. A comparison of detonation velocities obtained from the experiment and the simulation for various reaction rate parameters is shown in Table 2 and Fig. 3. Diameter effect on the detonation velocity is generally expressed by the relationship between the reciprocal

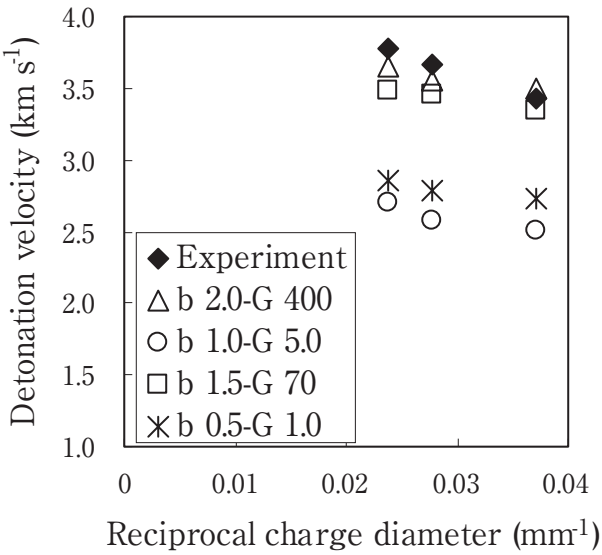

Fig. 3 Comparison of the detonation velocity of ANFO obtained by the experiment and the simulation. The filled diamonds are experimental values; the others are the simulation results with the values of the parameters variously changed. When the parameters b and G were set to 2.0 and 400, the simulated detonation velocities best fitted to experimental values.

diameter and the corresponding detonation velocity as shown in Fig. 3. Our previous experimental data have been plotted in Fig. 3 as symbol◆. The detonation velocity increases as the value of b decreases, and it increases as the value of G increases. When the reaction rate parameters b and G were set to 2.0 and 400, respectively, the simulated detonation velocities fitted best to the experimental values for all charge diameters. We use the numerical results that performed with these parameters in the following discussion.

Figure 4 shows the loci of the shock front by the 10 cm from the top end of the main part of ANFO obtained by the simulations for 27 and 42 mm diameter charges. Although two loci are almost the same by about 5 μs from the origin, the discrepancy can be seen after 5 μs. The shock front of the 27 mm diameter charge has a higher velocity than that of the 42 mm diameter charge. However, from about 13.6 μs, the shock front in the 42 mm diameter charge accelerates to approach a steady state detonation. The velocity of the steady detonation was examined by arrival time of shock front and distance between 100 mm

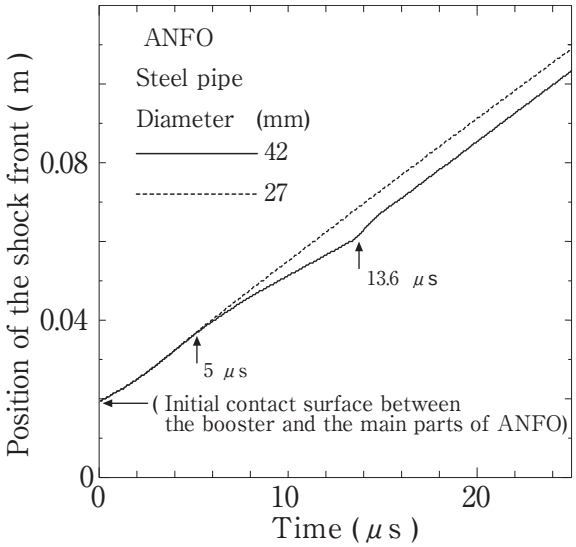

Fig. 4 The locus of the shock front obtained by the simulations.

to 300 mm from the top end of the main ANFO. It is found that the steady detonation velocity for the 42 mm charge is higher than that for the 27 mm charge. As the initiation condition is the same in each case, the difference in the detonation velocity is caused by the difference in the charge diameter. The simulation reproduces non−ideal behavior based on the effect of the diameter.

The profiles of the mass fraction of detonation products as a function of position are shown in Fig. 5. The corresponding values of the mass fraction at the sonic point are indicated by circles. At the sonic point, the mass fractions of product are quite high. However, the chemical reaction proceeds behind the sonic point, *i.e.*, a chemical reaction is not completed within the detonation driving zone. The sonic point is attained at a point 7.5 mm behind the detonation front. The length of the detonation driving zone is about 20% of the charge diameter. Figure 5 (a) shows a comparison of the mass fraction of detonation products along the axis and that along the charge periphery. These profiles are similar, however, and the detonation front at the charge periphery has a lag of 1mm from that at the axis, while the mass fraction of product in the axis is slightly higher. This trend is found for all charge diameter cases, however, the positions of the detonation front at the axis and the periphery are almost the same in the case of a 27 mm diameter charge. Figure 5 (b) shows the mass fraction of detonation products for 27 and 42 mm diameter charges. Although the length of the detonation driving zone is almost the same, the distribution of the mass fraction of detonation products is slightly different. From 0 to 0.6, the profiles of the mass fraction overlap each other. After that, a difference is noted, but this region is still in the detonation driving zone, and the reaction proceeds with the difference maintained after the detonation driving zone. The difference in the mass fraction at the sonic plane between the 27 and 42 mm cases is 8%. The difference in the detonation velocity of these cases is about 5%.

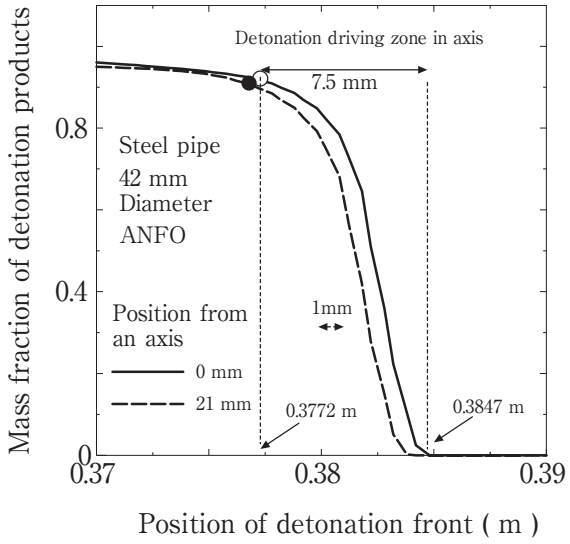

(a) Comparison of mass fraction of detonation products in the axis (solid line) and that in the periphery (dashed line). The detonation front at the charge periphery has a lag of 1mm from that at the axis. The circles show the corresponding values at the sonic point.

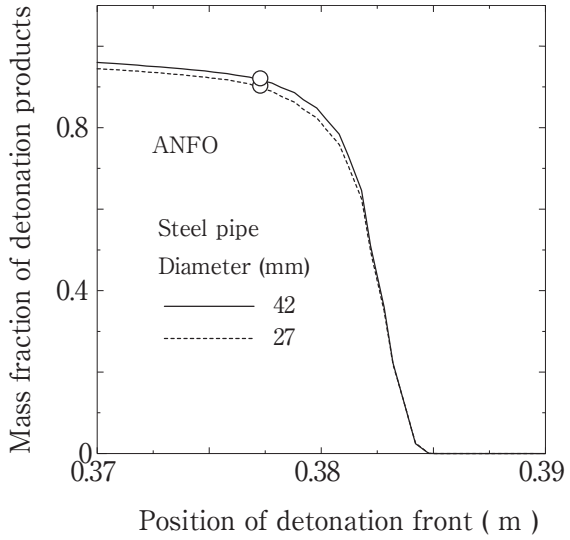

(b) Comparison of mass fraction of detonation products in the case of the charge diameter is 27 mm (dashed line) and 42 mm (solid line) in steady detonation wave. The circles show the values at the sonic point.

Fig. 5 Profiles of the mass fraction of detonation products in the steady detonation wave. The detonation propagation direction is right in the figure.

4. Conclusion

Numerical simulations of detonations of ANFO contained in a steel tube were carried out, and the corresponding experimental results were reproduced for the detonation velocities of 27, 36, and 42 mm diameter charges. The parameters of the reaction model that satisfied the experimental results were examined. The results were as follows. The curve of the detonation front was small. The length of the detonation driving zone was about 20% of the charge diameter. The lengths of the detonation driving zone were almost the same for each case. The slight difference in the distribution of the mass fraction of detonation products produced the difference in detonation velocity

References

1) M. A. Cook, The science of high explosives, Reinhold (1958)
2) A. Miyake, T. Ogawa, S. Saitoh, N. Yoshida, J. Ind. Explos. Soc. Jpn, 52, 336 (1991) (in Japanese)
3) A. Miyake, T. Ogawa, S. Saitoh, N. Yoshida, ibid., 53, 67 (1992) (in Japanese)
4) A. Miyake, K. Takahara, T. Ogawa, Y. Ogata, Y. Wada, H. Arai, J. Loss Prev. Proc. Ind., 14, 533 (2001)
5) A. Miyake, K. Takahara, T. Ogawa, Y. Ogata, H. Arai, J. Ind. Explos. Soc. Jpn, 63, 279 (2002) (in Japanese)
6) H. Arai, Y. Ogata, Y. Wada, A. Miyake, W. Jun, J. Nakamura, T. Ogawa, Sci. Tech. Energetic Materials, 65, 201 (2004)
7) A. Miyake, H. Kobayashi, H. Echigoya, S. Kubota, H. Arai, Y. Ogata, Y. Wada, T. Ogawa, J. Loss Prev. Proc. Ind., 20, 584 (2007)
8) P. C. Souers, S. Anderson, J. Mercer, E. McGuire, P. Vitello, Propellants, Explos., Pyrotech., 25, 54 (2000)
9) Z. Liu, S. Kubota, M. Otsuki, K. Yoshimura, K. Okada, Y. Nakayama, M. Yoshida, S. Fujiwara, J. Ind. Explos. Soc. Jpn, 63, 264 (2002)
10) S. Kubota, T. Saburi, Y. Ogata, and K. Nagayama, Sci. Tech. Energetic Materials, 71, 44 (2010)
11) S. Kubota, T. Saburi, Y. Ogata, and K. Nagayama, Sci. Tech. Energetic Materials, 71, 92 (2010)

鋼管中に装填されたANFO爆薬の爆速および反応帯に対する薬径の影響

木下直樹*，久保田士郎，佐分利禎**，緒方雄二**，三宅淳巳*†**

硝安を主成分とする非理想爆薬の爆轟特性に関する知見を得るために，Euler流体解析コードを用いてANFO爆薬の爆轟の数値シミュレーションを行い，爆轟実験結果との比較を行った。シミュレーションによって，各薬径におけるANFO爆薬の爆速の実験値が再現された。またシミュレーションにおいては，爆轟波の先端の衝撃波面はわずかに湾曲を呈した。爆轟波中の爆轟生成物の分布は薬径ごとに異なっており，爆薬の中心部と側端部とでもわずかに違いが見られた。

*横浜国立大学大学院環境情報学府　〒240−8501　横浜市保土ヶ谷区常盤台79－７
TEL 045−339−3993　FAX 045−339−4011
†Corresponding address atsumi@ynu.ac.jp

**独立行政法人産業技術総合研究所安全科学研究部門爆発安全研究コア　〒305−8569　つくば市小野川16−１
e−mail kubota.46@aist.go.jp